The 10th International Topical Meeting on Nuclear Reactor Thermal Hydraulics (NURETH-10)
Seoul, Korea, October 5-9, 2003.

CHARACTERISTIC AND PROPAGATION VELOCITIES OF THE TWO-FLUID MODELS

Iztok Tiselj, Janez Gale, Andrej Horvat, Iztok Parzer
"Jožef Stefan" Institute, Reactor Engineering Division
Jamova 39, 1000, Ljubljana, Slovenia
iztok.tiselj@ijs.si, janez.gale@ijs.si
andrej.horvat@ijs.si, iztok.parzer@ijs.si

KEY WORDS

two-fluid model, hyperbolic equations, relaxation terms

ABSTRACT

Influence of the stiff inter-phase exchange source terms on the propagation velocities of the two-fluid models is analyzed. If infinitely fast inter-phase exchange is assumed, i.e. instantaneous thermal and mechanical relaxation, the results of the two-fluid models should be similar to the results homogeneous-equilibrium model, despite different characteristic velocities of both models. Results of the present work show, that the propagation velocities of the two-fluid model with infinitely stiff relaxation terms are indeed equal to the propagation velocities of the homogeneous-equilibrium model - despite large differences in the eigen-structures of the two-fluid models and HEM model. It is known that the speed of sound in two-fluid model is not the same as the HEM speed of sound, however, the propagation speed of the sonic waves of the two-fluid models with infinitely stiff relaxation terms is close to the HEM speed of sound and not the speed of sound of the two-fluid model. For non-stiff relaxation source terms the characteristic velocities of the two-fluid model are approximately equal to the wave propagation velocities.

1. INTRODUCTION

Typical two-fluid model used in computer codes like RELAP5 (Carlson et al., 1990), TRAC (Mahaffy, 1993) or Cathare (Bestion, 1990) can be written as:

$$\underline{A}\,\frac{\partial \vec{\psi}}{\partial t} + \underline{B}\,\frac{\partial \vec{\psi}}{\partial x} = \vec{S} \quad , \tag{1}$$

Similar two-fluid model is used in computer code WAHA, which is being developed as a part of WAHALoads project within the 5th research program of the European Union (Giot et. al. 2001, Tiselj et. al. 2003), with a goal to simulate water hammer transients in the nuclear systems. The two-fluid models in the above mentioned codes describe two-phase flow of water with six equations: mass, momentum and energy balances for vapor and liquid. Differential terms are collected on the left-hand side of the

equations and the non-differential terms are collected on the right. Source terms in vector $\vec{S}$ can be divided into two groups:

- Inter-phase exchange source terms (relaxation source terms) - $\vec{S}_R$ - terms describing inter-phase mass, momentum, and energy transfer, which tend to establish mechanical ($v_r \to 0$) and thermal equilibrium ($T_f, T_g \to T_s$). Characteristic time scale of these relaxation source terms can be much shorter than the characteristic time scale of the acoustic waves, thus, these source terms are often stiff.
- Other source terms $\vec{S}_{N-R}$: wall friction, volumetric forces, and wall-to-heat transfer source terms are not relaxation sources, however they have characteristic time scale longer than that of the acoustic waves and they seldom present problems for the numerical schemes.

A lot of work has been done in the past few years in the field of the numerical solutions of the hyperbolic part of the equation, which are based on the evaluation of the characteristic velocities of the two-fluid models (Toumi, Kumbaro, 1996, Tiselj, Petelin, 1997, or Evje, Fjelde, 2002 ...). Most of that work was focused on the solution of the hyperbolic part of the two-fluid model (Eq. (1) without source terms), while only a small part of attention was focused on the source terms. These numerical schemes present an extension of similar schemes developed for simulations of single-phase compressible flows (Euler equations).

One of the main differences between the Euler equations of ideal gas flow and equations of two-fluid models: characteristic velocities are propagation velocities of the waves in single-phase compressible flow, however, characteristic velocities of the two-fluid models of two-phase flow are not necessarily the propagation velocities.

Results of the present paper show the influence of the stiff inter-phase exchange source terms on the propagation velocities of the two-fluid models. When infinitely fast inter-phase exchange is assumed in the two-fluid model, i.e. instantaneous thermal and mechanical relaxation, the results of the two-fluid models are similar to the results homogeneous-equilibrium model (HEM model), despite different characteristic velocities of both models. Results of the present work show, that the propagation velocities of the two-fluid model with infinitely stiff relaxation terms are indeed equal to the propagation velocities of the homogeneous-equilibrium model - despite large differences in the eigen-structures of the two-fluid models and HEM model.

2. TWO-FLUID MODEL EQUATIONS

Results in the present paper were obtained with WAHA computer code (Giot et. al. 2001, Tiselj et. al. 2003) that solves hyperbolic equations. The numerical scheme applied is based on the Godunov method. Its behavior with the equations of the two-fluid models was analyzed by Tiselj and Petelin (1997) while the brief description of the numerics is given in the next section. Mathematical model considered in this paper is six-equation two-fluid model similar to the models of RELAP, TRAC, or Cathare computer codes. The basic equations are mass, momentum and energy balances for vapor and liquid, without terms for wall-to-fluid heat transfer:

$$\frac{\partial A(1-\alpha)\rho_f}{\partial t} + \frac{\partial A(1-\alpha)\rho_f v_f}{\partial x} = -A\Gamma_g \tag{1}$$

$$\frac{\partial A\alpha\rho_g}{\partial t} + \frac{\partial A\alpha\rho_g v_g}{\partial x} = A\Gamma_g \tag{2}$$

$$\frac{\partial A(1-\alpha)\rho_f v_f}{\partial t} + \frac{\partial A(1-\alpha)\rho_f v_f^2}{\partial x} + A(1-\alpha)\frac{\partial p}{\partial x} - A*CVM - Ap_i\frac{\partial \alpha}{\partial x} = AC_i|v_r|v_r - A\Gamma_g v_i + A(1-\alpha)\rho_f g\cos\theta - AF_{f,wall} \tag{3}$$

$$\frac{\partial A\alpha\,\rho_g v_g}{\partial t} + \frac{\partial A\alpha\,\rho_g v_g^{\,2}}{\partial x} + A\alpha\frac{\partial p}{\partial x} + A^{*}\,CVM + Ap_i\frac{\partial \alpha}{\partial x} = \tag{4}$$
$$-AC_i\,|v_r|\,v_r + A\Gamma_g v_i + A\alpha\rho_g g\cos\theta - AF_{g,wall}$$

$$\frac{\partial A(1-\alpha)\,\rho_f e_f}{\partial t} + \frac{\partial A(1-\alpha)\,\rho_f e_f v_f}{\partial x} + p\frac{\partial A(1-\alpha)}{\partial t} + \frac{\partial A(1-\alpha)\,pv_f}{\partial x} = \tag{5}$$
$$AQ_{if} - A\Gamma_g(h_f^{*} + v_f^2/2) + A(1-\alpha)\rho_f g\cos\theta\, v_f$$

$$\frac{\partial A\alpha\,\rho_g e_g}{\partial t} + \frac{\partial A\alpha\,\rho_g e_g v_g}{\partial x} + p\frac{\partial A\alpha}{\partial t} + \frac{\partial A\alpha\,pv_g}{\partial x} = \tag{6}$$
$$AQ_{ig} + A\Gamma_g(h_g^{*} + v_g^2/2) + A\alpha\rho_g g\cos\theta\, v_g$$

Specific total energy of liquid or gas is:

$$e = u + v^2/2 \tag{7}$$

and specific enthalpy of liquid or gas is:

$$h = u + p/\rho \tag{8}$$

Differential terms are collected on the left-hand side of the equations and the non-differential terms are collected on the right. Pipe cross-section A can vary as a function of coordinate x and time:

$$A(x,t) = A(x) + A_e(p(x,t))\,, \qquad \frac{dA_e}{A(x)} = \frac{D}{d}\frac{dp}{E} = K\,dp \tag{9}$$

The A_e terms take into account elasticity of the pipe walls, which modifies the propagation velocities in the elastic pipes and is especially important when modeling water hammer transients. Pipe elasticity is not taken into account in the present work.

Additional closure relations needed:

1) Two additional equations of state for each phase are needed. The equation of state for phase k is

$$d\,\rho_k = \left(\frac{\partial \rho_k}{\partial p}\right)_{u_k} d\,p + \left(\frac{\partial \rho_k}{\partial u_k}\right)_{p} du_k \quad . \tag{10}$$

Derivatives on the right hand side of the Eq. (10) are determined by the water property subroutines developed for WAHA code using pressure and temperature or specific internal energy as input. Water properties are pre-tabulated and saved at approximately 400 pressures and 400 temperatures. Densities are treated as a continuous piecewise linear functions of p and u_k (or T_k), with discontinuous derivatives (details in Tiselj et. al. 2003).

2) The virtual mass term CVM in Eqs. (3) and (4) is used to obtain hyperbolicity of equations:

$$CVM = (1-S)C_{vm}\,\alpha\,(1-\alpha)\,\rho_m\left(\frac{\partial v_g}{\partial t} + v_f\frac{\partial v_g}{\partial x} - \frac{\partial v_f}{\partial t} - v_g\frac{\partial v_f}{\partial x}\right) \tag{11}$$

Value of coefficient C_{vm} was tuned to ensure the hyperbolicity of the two-fluid model equations (see Tiselj, Petelin, 1997 for details). It worths to mention that applied virtual mass term does not ensure unconditional hyperbolicity of the equations. For very large relative velocities (comparable to sonic velocity) complex eigenvalues may appear, however these are extremely rare occasions.

3) Interfacial pressure term exists only in stratified flow:

$$p_i = S\alpha(1-\alpha)(\rho_f - \rho_g)gD \tag{12}$$

where S presents the stratification factor ($S=0$ for dispersed flow, $S=1$ for horizontally stratified flow, $0<S<1$ for transitional flow - see Tiselj et. al. 2003 for details).

4) WAHA code distinguishes two flow regimes: dispersed and horizontally stratified with transition area between both regimes. Source terms are flow regime dependent and their detailed form is given in the WAHA manual (Tiselj et. al. 2003). Terms that do not include derivatives - source terms - are:
   - 4.1) Terms with C_i - inter-phase drag.
   - 4.2) Terms with Γ_g, Q_{ig}, Q_{if} - inter-phase exchange of mass and energy with:
     $\Gamma_g=-(Q_{if}+Q_{ig})/(h_g-h_f)$ - vapor generation term,
     $Q_{if}=H_{if}(T_s-T_f)$, $Q_{ig}=H_{ig}(T_s-T_g)$ - interface heat transfer terms,
     H_{if}, H_{ig} - liquid-interface and gas-interface heat transfer coefficients.
   - 4.3) Terms due to the variable pipe cross-section.
   - 4.4) $F_{f,wall}$, $F_{g,wall}$ - wall friction.
   - 4.5) Term with $g\cos\theta$ - volumetric forces.
   - 4.6) Terms for wall heat transfer and mass and momentum exchange due to the boiling or condensation on the wall - these sources are neglected in WAHA code.

Sources from the points 4.1) and 4.2) are the so-called relaxation source terms: inter-phase mass, momentum, and energy exchange terms, which tend to establish thermal and mechanical equilibrium between the phases. Characteristic time scale of these source terms can be much shorter than the characteristic time scale of the acoustic waves. These are stiff source terms that require special numerical treatment.

Other source terms: wall friction, volumetric forces, and wall-to-heat transfer source terms are not relaxation sources, however they have characteristic time scale longer than that of the acoustic waves and they seldom present problems for the numerical schemes.

2. NUMERICAL METHOD

The numerical scheme of WAHA code is based on the characteristic upwind method. Its behavior with the equations of the two-fluid models was analyzed by Tiselj and Petelin (1997) while a brief description of the numerics is given below. The system of equations (1)-(6) can be written in the following non-conservative form, which is suitable for the numerical solving:

$$\underline{A}\,\frac{\partial\vec{\psi}}{\partial t} + \underline{B}\,\frac{\partial\vec{\psi}}{\partial x} = \vec{S} \ , \tag{13}$$

where $\vec{\psi}$ represents the vector of the independent variables $\vec{\psi} = (p, \alpha, v_f, v_g, u_f, u_g)$, $\underline{A}$ and $\underline{B}$ are matrices of the system, and $\vec{S}$ is a vector with non-differential terms in the equations. The numerical scheme used in 2F code is a two-step scheme with operator splitting; i.e. convection with non-relaxation source terms $\vec{S}_{N-R}$ and relaxation sources $\vec{S}_R$ in Eq. (13) are treated separately:

$$\underline{A}\,\frac{\partial\vec{\psi}}{\partial t} + \underline{B}\,\frac{\partial\vec{\psi}}{\partial x} = \vec{S}_{N-R} \ , \tag{14}$$

$$\underline{A}\,\frac{d\vec{\psi}}{dt} = \vec{S}_R \ , \tag{15}$$

One time step includes the following two sub-steps (superscripts $n, n+1$ denote time levels - * denotes intermediate time level):

1) - Convection terms and non-relaxation sources - Eq. (14):

$$\vec{\psi}_j^{*} = \vec{\psi}_j^{n} - \Delta t \left(\left(\underline{A}^{-1} \vec{S}_{N-R} \right) + \left(\underline{A}^{-1} \underline{B} \right) \frac{\partial \vec{\psi}^{n}}{\partial x} \right)_j \tag{16}$$

2) - Integration of the relaxation sources - Eq. (15) :

$$\vec{\psi}_j^{n+1} = \vec{\psi}_j^{*} + \int_{t^*}^{t^*+\Delta t} \underline{A}^{-1}(\vec{\psi}_j{}^{*}(t)) \vec{S}_R(\vec{\psi}_j{}^{*}(t)) \, dt \tag{17}$$

Step 1) Eq. (16) is solved with second-order accurate characteristic upwind scheme that requires hyperbolicity of the equations. Eigenvalues and eigenvectors are explicitly calculated:

$$\underline{A}^{-1}\underline{B} = \underline{L} \cdot \underline{\Lambda} \cdot \underline{L^{-1}} \tag{18}$$

and upwind discretisation is used for each characteristic equation. Second-order accuracy is achieved with slope limiters. Algorithm for integration of non-relaxation source terms is described in Tiselj et. al. 2003.

Step 2) Eq. (17) is integrated over the Δt (convective time step) with first-order explicit method in each grid point. Time steps of the integration depend on the stiffness of the relaxations and can be much shorter that the main time step Δt. First-order accuracy of this sub-step is compensated by the shorter time steps in integration of Eq. (17). Another option is available in WAHA code - instantaneous relaxation of the source terms in Eq. (17). An assumption in that case is that the inter-phase exchange processes are infinitely fast. Integration of Eq. (17) with infinite values of inter-phase friction (C_i), and liquid-interface and gas-interface heat transfer coefficients (H_{if}, H_{ig}) is not possible, however, the relaxed state can be found directly: both phasic velocities become equal to the mixture velocity and the phasic properties (densities, internal energies) become equal to the equilibrium properties. Properties of the thermal equilibrium are calculated from the given mixture density and mixture internal energy.

The operator splitting given by Eqs. (16) and (17) is formally first-order accurate. However, the numerical tests have shown, that despite the formally lower order of accuracy, the results are practically the same as with the second-order accurate Strang splitting (Le Veque, 1992).

Numerical scheme of WAHA code is non-conservative (see vector of the independent variables $\vec{\psi}$ near Eq. 13). Non-conservative schemes are known to converge to the wrong solutions when shocks are present in the flow field (see Tiselj , Petelin, 1997), however, in typical single-phase water hammer transients, these "wrong" solutions are very close to the exact solutions. In two-phase flows, shock waves are actually not discontinuities and their velocities are not well known, thus, errors due to the non-conservative numerics are much lower than non-accuracy of the applied physical models. According to the present experience, non-conservative scheme does not seem to be a big deficiency for short transients like water hammer events.

4. RESULTS

This section shows numerical results for two cases:

- In sub-section 4.1 the two-phase shock tube problem is solved with WAHA code with several different values of inter-phase exchange coefficients C_i, H_{if}, H_{ig} in relaxation source terms. WAHA results are compared with results of the homogeneous equilibrium model (HEM) of two-phase flow, with neglected wall friction, volumetric forces and wall-to-fluid heat transfer:

$$\frac{\partial \rho_m}{\partial t} + \frac{\partial \rho_m v_m}{\partial x} = 0 \tag{19}$$

$$\rho_m \frac{\partial v_m}{\partial t} + \frac{1}{2}\rho_m \frac{\partial v_m^2}{\partial x} + \frac{\partial p}{\partial x} = 0 \tag{20}$$

$$\frac{\partial \rho_m u_m}{\partial t} + \frac{\partial \rho_m u_m v_m}{\partial x} + p\frac{\partial v_m}{\partial x} = 0 \tag{21}$$

- In sub-section 4.2 the two-phase critical flashing flow in convergent-divergent nozzle is simulated with WAHA code and with RELAP5 code with HEM options switched on and choking option switched of.

4.1 Shock tube

Two-phase shock-tube is Riemann problem for the two-fluid model: a single discontinuity in 1D. Results in Fig. 1 are for the following initial conditions:

x<50 m: p=15 MPa, α=0.1, v_f=v_g=0.0, T_f=T_g=615.3 K
x>50 m: p=10 MPa, α=0.5, v_f=v_g=0.0, T_f=T_g=584.2 K

As can be noticed, the phasic temperatures and phasic velocities on both sides are equal, thus the initial state can be used as input for six-equation WAHA model and for HEM model.

Figures 1 and 2 present a series of five simulations with the two-fluid model (WAHA code) and one simulation with the HEM model ("home-made" code), on coarse (100 nodes) and fine (2500 nodes) grids, respectively. Results are presented at time t=0.081 s. Calculations with two-fluid model were performed with different various coefficients C_i, H_{if}, H_{ig} - values of the coefficients are written in each graph of the Figs. 1 and 2. Stratification factor (Eqs. (10), (11)) was set to $S=0$, i.e., the virtual mass term was used in equations, while the interfacial pressure was zero. It is important to stress that virtual mass presents significant inter-phase friction, which is present in all simulations. Results present phasic velocities in the left and phasic temperatures in the right column. No inter-phase exchange was allowed in the first simulation (Figs. 1 and 2, first row) and one can see a significant difference between the solutions of the two-fluid model and the solutions of the HEM model. Shocks traveling right and rarefaction waves traveling left are much faster in two-fluid model than in the HEM model. Discontinuity in the middle of the tube that exists in two-fluid model solutions does not exist in HEM solutions. Larger coefficients are used in the next simulation (second row in Figs. 1, 2): one can see that the phasic velocities are closer now, while the phasic temperatures are still far away. In the third simulation (third rows in Figs. 1, 2) the phasic velocities are quite close, while the temperatures are still quite different. Here it can be seen that discontinuities of the two-fluid model become very smeared: instead of the sharp shocks, rarefaction waves and contact discontinuities, the waves are interlaced. The phasic velocities and temperatures are very close together in the fourth simulation (fourth rows in Figs. 1, 2) and also close to the solutions of the HEM model. When the coefficients are increased further (bottom row in Figs. 1, 2) - we obtain a two-fluid model with extremely high inter-phase mass, momentum and energy transfer, which is practically equal to the three-equation HEM model. Coarse grid (bottom row in Fig. 1) results obtained with $C_i=10^6$ and $H_{if}=H_{ig}=10^9$ are practically the same as results obtained with infinite values of the coefficients. On finer grid (Fig. 2 bottom) a small, but visible difference between $C_i=10^6$ and $H_{if}=H_{ig}=10^9$ results and infinite values exists: results are plotted for $C_i=\infty$ and $H_{if}=H_{ig}=\infty$ as WAHA code allows "infinite coefficients, i.e. instantaneous relaxation.

It can be noticed in the bottom row of Fig. 1 that solution of the WAHA code with very large values of coefficients (infinite) is more "diffusive" than the HEM solution. The same effect is present on fine grid but barely seen in the bottom row of the Fig. 2. This is due to the non-accuracy of the operator splitting technique (see Tiselj, Horvat, 2002 for details).

Comparison of Figs. 1 and 2 shows that computations are practically "grid independent" with the same intermediate states on coarse and fine grids.

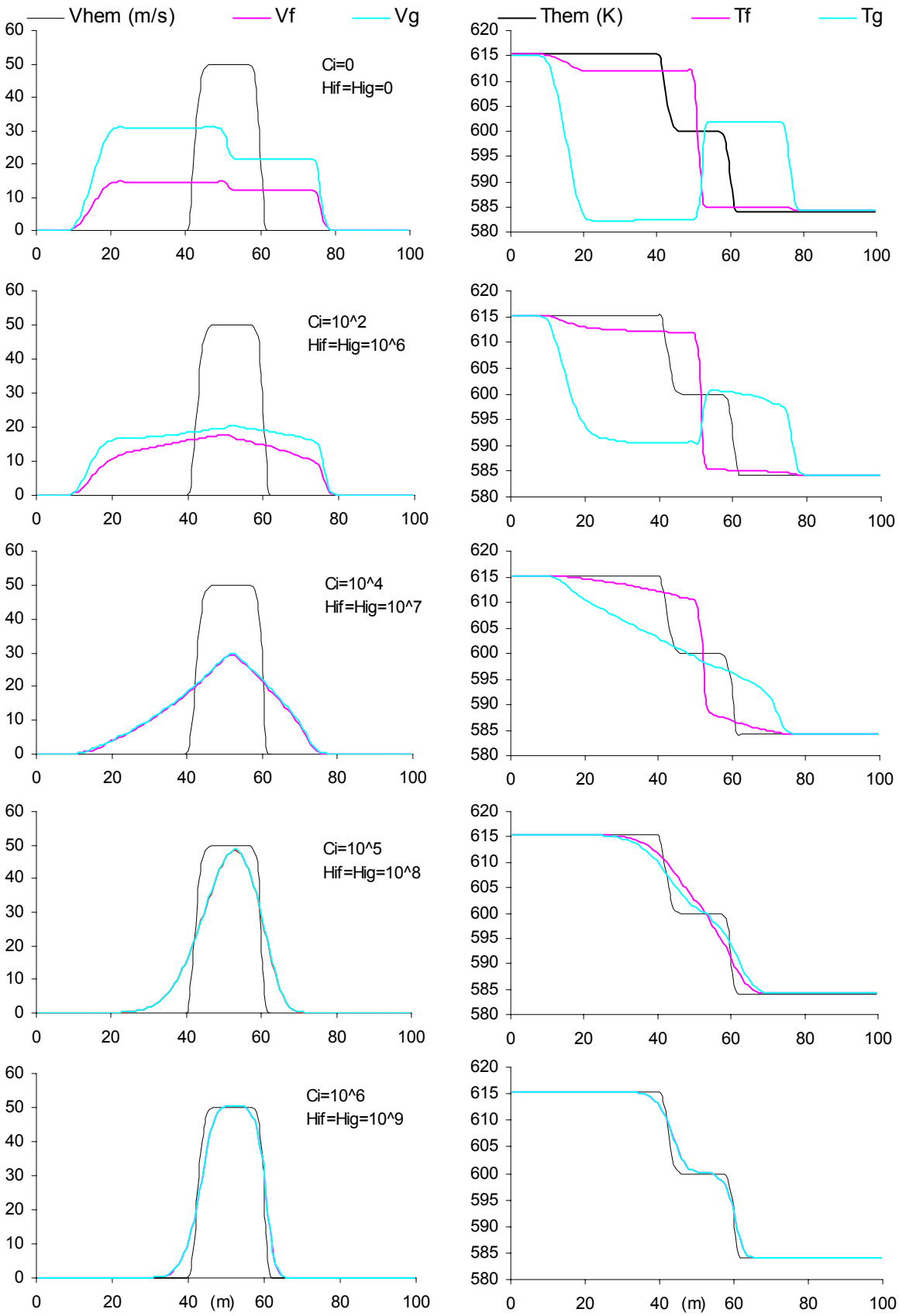

Fig. 1: Phasic velocities v_f, v_g and phasic temperatures T_f, T_g of two-fluid models converge toward the values predicted by HEM model, as the inter-phase drag coefficient (C_i) and heat transfer coefficients (H_{if} , H_{ig}) are increased. Propagation velocities of two-fluid model also strongly depend on the strength of the relaxation source terms. Coarse grid results (100 nodes).

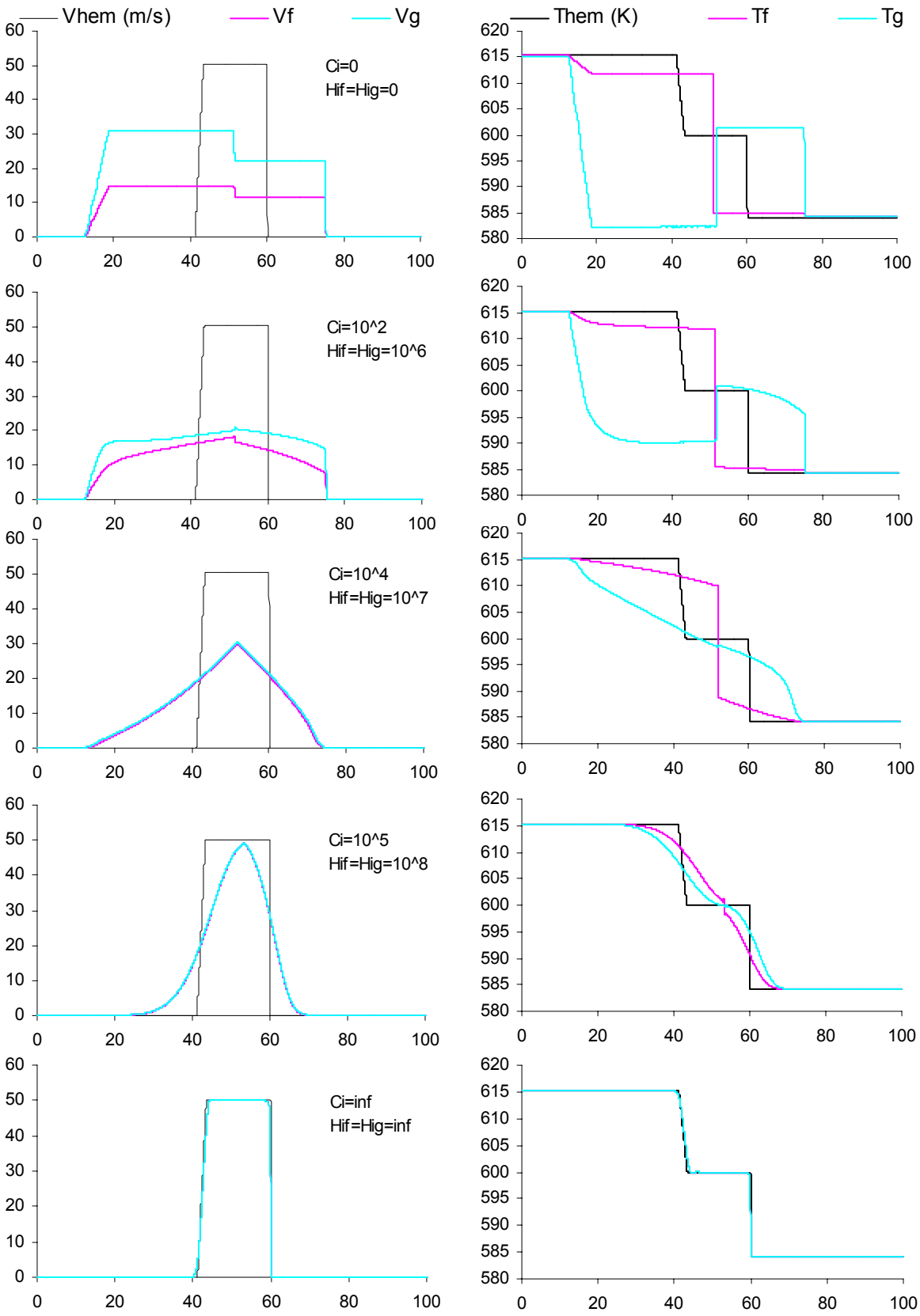

Fig. 2: Phasic velocities v_f, v_g and phasic temperatures T_f, T_g of two-fluid models converge toward the values predicted by HEM model, as the inter-phase drag coefficient (C_i) and heat transfer coefficients (H_{if} , H_{ig}) are increased. Propagation velocities of two-fluid model also strongly depend on the strength of the relaxation source terms. Fine grid results (2500 nodes).

Results shown in Figs. 1, 2 raise the question of the importance of the eigenvalues of the two-fluid model and numerical schemes based on characteristic decomposition. Accurate prediction of eigenvalues is certainly important at low rates of, heat, mass and momentum transfer. However, significant inter-phase transfer exists in most relevant situations in two-phase flow, and eigen-structure of the two-fluid model is certainly not very important in such cases.

4.2 Critical flow in convergent-divergent nozzle

This section presents results obtained for two-phase flashing flow in a convergent-divergent nozzle of cross-section (Anderson, 1995):

$$A(x) = 1. + 2.2*(x-1.5)^2, \qquad 0 \le x \le 3m. \tag{22}$$

Nozzle is shown in Fig. 3. The calculations have been performed with WAHA code and with RELAP5/MOD3 code. Wall friction was switched of in all WAHA and RELAP5 simulations. RELAP5 is based on six-equation two-fluid model, but due to the numerical limitations cannot perform simulations of two-phase critical flow directly with six-equation two-fluid model, and is using special "choking" models for critical flow simulations. In the present work RELAP5 was used without special model ("choking" was disabled) and the flow was simulated as homogeneous equilibrium, i.e. HEM model in RELAP5 was used (simple home-made HEM code used in the previous shock-tube section was not used in this section because it does not allow area changes).

WAHA code was not intended to be used for direct modeling of two-phase critical flows (most of the water hammer's are low velocity phenomena), however it can simulate such transient. Simulation was performed with instantaneous relaxation of inter-phase heat, mass, and momentum transfer. The following boundary conditions were used:

- inlet: p=2 bar, T=392.9 K, $\alpha = 0$
- outlet: p=1 bar

Initial conditions were: v_f=v_g=0 and $\alpha = 0$, transient was running until the steady state critical flow was reached. Nozzle was discretized in 51 cells. Due to the single-phase liquid and slight subcooling (0.5 K) at the inlet, the steady-state flow is single phase in the first part of the pipe and flashing appears before the nozzle throat. Figure 4 shows the pressure profiles in the nozzle, Fig. 5 vapor volume fraction profiles, and Fig. 6 shows mass flow rate profiles.

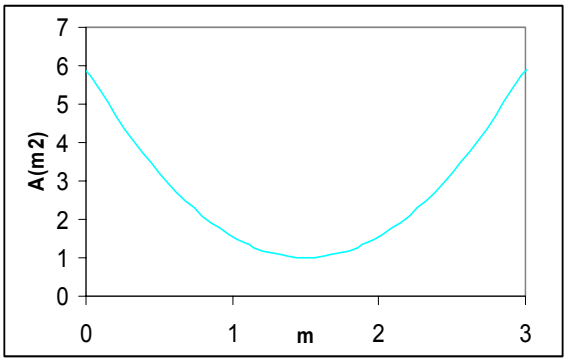

Fig. 3: Nozzle cross-section

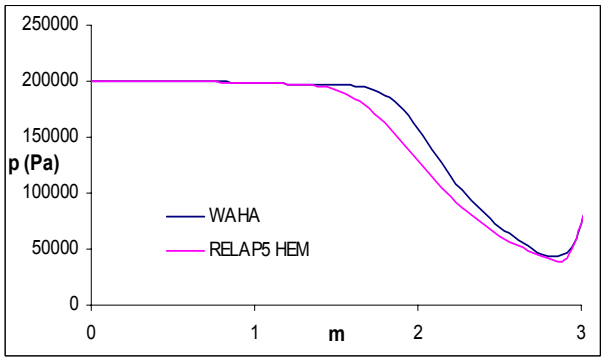

Fig. 4: Steady-state pressure profile in the nozzle.

One could expect higher critical flow rate predicted by two-fluid model that by HEM model, because the sonic velocity of the two-fluid model is larger than the sonic velocity of the HEM model. However, like in the previous section, very similar results are obtained with HEM model from RELAP5 and WAHA code with instantaneous relaxation. The fact is that WAHA code does not know anything about the HEM sound velocity - it's eigenvalues are different than eigenvalues of the HEM

model, but the present results show that the flow becomes "choked" approximately when mixture velocity exceeds the local HEM speed of sound. If we define choking as a point where the mixture velocity exceeds the local speed of sound, then the WAHA flow is not choked at all, because the mixture velocity never exceeds the sonic velocity of the two-fluid model. However, the flow is choked if we define choking as a flow rate, which does not depend on the downstream pressure. This is shown in Fig. 7 where mixture velocities calculated with RELAP5-HEM are compared with results of WAHA with instantaneous relaxation ("quasi-HEM" WAHA). Fig. 7 shows also local HEM speed of sound calculated by RELAP5 HEM, and speed of sound of the WAHA calculation. Mixture velocities never exceed the two-fluid speed of sound, but do exceed the HEM speed of sound.

Figs. 6 and 8 show the non-negligible rate of mass non-conservation in WAHA code for the problem with flashing flow in the nozzle: maximal mass error is 4% in Fig. 6 and 12% in Fig. 8 (case WAHA CORR.). Nozzle flow calculated with WAHA correlations (WAHA CORR. case in Fig. 8) is not perfectly steady but is fluctuating in time. If temporal average of the mass flow rate profile is calculated, the maximal mass error is approximately 5%. However, non-conservation of mass (energy and momentum) in the nozzle is still at least an order of magnitude higher than non-conservation in typical water hammer problems.

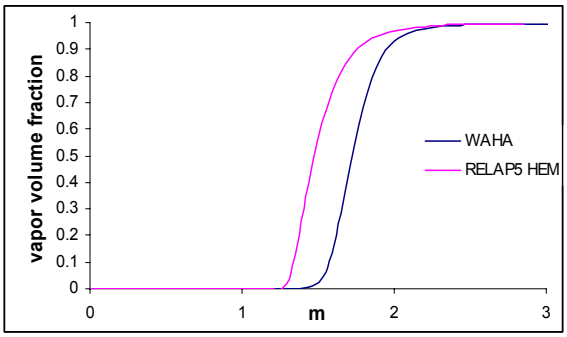

Fig. 5: Vapor volume fraction profile.

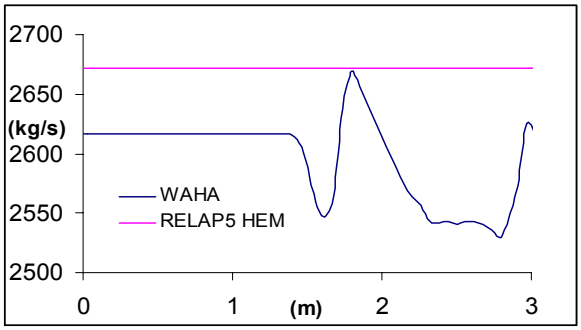

Fig. 6: Mass flow rate profile.

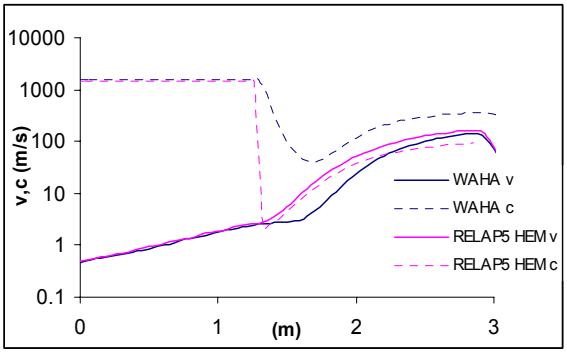

Fig. 7: Mixture velocity profiles, HEM speed of sound, two-fluid model speed of sound.

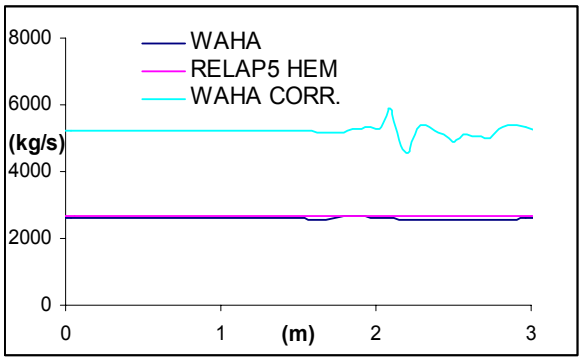

Fig. 8: Mass flow rate profiles: WAHA CORR. profile obtained with WAHA code and built-in correlations.

It is interesting to add that critical flow predicted with built in WAHA correlations, is roughly two times larger that the HEM critical flow of RELAP5 and "quasi-HEM" critical flow from WAHA code (Fig. 8). As the WAHA correlations for inter-phase heat, mass, and momentum transport are not fixed yet, "WAHA CORR." profile in Fig. 8 should be taken as preliminary result.

Similar study with variation of the inter-phase exchange coefficients, like in the shock tube case, would be possible with nozzle case too, however, the simulation would fail at low inter-phase fricton

coefficients, due to the very high relative velocities, where equations of the two-fluid model become non-hyperbolic.

Like the shock tube problem, the critical flow case again diminishes the role of the eigenvalues of the two-fluid model and shows a significant influence of the relaxation source terms (inter-phase exchange source terms) on the propagation velocities of the system.

5. CONCLUSIONS

The present work describes the relation between the eigenvalues of the hyperbolic six-equation two-fluid modes and relaxation source terms that describe inter-phase exchange of mass, momentum and energy. Results show that solutions of the applied six-equation two-fluid model tend to the solutions of the three-equation homogeneous-equilibrium model as the strength (stiffness) of the relaxation source terms is increased. It is well known that the inter-phase exchange source terms can be stiff. i.e. their characteristic time scale can be very short, much shorter than the characteristic time scale of the acoustic waves. This stiffness is responsible for the influence of the relaxation source terms on the propagation velocities of the two-fluid models.

These findings should be taken into account in the field of numerical schemes for two-fluid models, where probably too much attention has been devoted to the accurate evaluation of the eigen-structure of the two-fluid models in the past. Schemes, which do not depend on the exact eigen-structure (AUSM schemes for example - see Paillere 2002 for example), might be found as sufficiently accurate for simulations of two-phase flows.

NOMENCLATURE

p pressure (Pa)
α vapor volume fraction (m^3/m^3)
v velocity (m/s)
u specific internal energy (J/kg)
e specific total energy (J/kg)
ρ density (kg/m^3)
s specific entropy (J/kg K)
T temperature (K)
Γ_g vapor source term (kg/s/m3)
C_{vm} virtual mass coefficient.
CVM virtual mass term
C_i inter-phase drag coefficient (kg/m4)
v_i velocity of the interface
θ inclination of the pipe
h specific internal enthalpy (J/kg)
H_i heat transfer coefficient (W/m3/K)
Q_{if}, Q_{ig} heat fluxes from interface to phase f or g
A pipe cross-section (m2)
p_i interfacial pressure
E pipe elasticity module
D pipe diameter
d pipe wall thickness
S stratification factor

Vectors and matrices:
$\underline{\mathbf{A}}$ matrix - temporal derivatives

$\underline{\mathbf{B}}$ matrix - spatial derivatives
$\vec{S}$ vector - sources
$\vec{\psi}$ independent variables
$\underline{\mathbf{\Lambda}}$ eigenvalues matrix
$\underline{\mathbf{L}}$ eigenvectors matrix

Subscripts
f liquid
g vapor
m mixture
s saturation
i interface

ACKNOWLEDGEMENT

Authors were supported by the Ministry of Education, Science and Sport of Republic of Slovenia and within the WAHALoads project of the 5th Framework Programme of European Union - Euratom.

REFERENCES

1. J. D. Anderson, *Computational Fluid Dynamics*, McGraw-Hill, New York, (1995)
2. D. Bestion, The Physical closure laws in the CATHARE code, *Nuclear Engineering and Design*, **124**, 229-245, (1990)
3. K.E. Carlson, R.A. Riemke, S.Z. Rouhani, R.W. Shumway, W.L. Weaver, *RELAP5/MOD3 Code Manual, Vol. 1-7*, **NUREG/CR-5535**, EG&G Idaho, Idaho Falls, 1990.
4. S. Evje, K. K. Fjelde , Hybrid Flux-Splitting Schemes for a Two-Phase Flow Model, *Journal of Computational Physics*, **175(2)**, 674-701 (2002).
5. M. Giot, H.M. Prasser, A. Dudlik, G. Ezsol, M. Habip, H. Lemonnier, I. Tiselj, F. Castrillo, W. Van Hove, R. Perezagua, S. Potapov, two-phase flow water hammer transients and induced loads on materials and structures of nuclear power plants (WAHALoads), *FISA 2001 EU research in reactor safety - Proceedings,* (2001).
6. R. J. LeVeque, Numerical Methods for Conservation Laws, *Lectures in Mathematics, ETH, Zurich*, (1992).
7. J. H. Mahaffy, Numerics of Codes: Stability, Diffusion, and Convergence, *Nuclear Engineering and Design* **145**, (1993)
8. H. Paillere, C. Corre and J. R. García Cascales, On the extension of the AUSM+ scheme to compressible two-fluid models, *Computers & Fluids*, **32(6)**, 891-916, (2003).
9. R. B. Pember, Numerical Methods for Hyperbolic Conservation Laws with Stiff Relaxation I. Spurious Solutions", *SIAM J. Appl. Math.* **53**, No. 5, 1293 (1993)
10. I. Tiselj, S. Petelin, 1997. Modelling of Two-Phase Flow with Second-Order Accurate Scheme. *Journal of Computational Physics*, **136**, 503-521 (1997).
11. I. Tiselj, A. Horvat, Accuracy of the operator splitting technique for two-phase flow with stiff source terms, *Proceedings of ASME Joint U.S.-European Fluids Engineering Conference*, Montreal, (2002).
12. I. Tiselj, G. Černe, A. Horvat, J. Gale, I. Parzer, M. Giot, J. M. Seynhaeve, B. Kucienska, H. Lemonnier, WAHA code manual, to be released in September 2003.
13. I. Toumi, A. Kumbaro, An Approximate Linearized Riemann Solver for a Two-Fluid Model", *Journal of Computational Physics,* **124**, 286 (1996).